

A Role for Methyl-CpG Binding Domain Protein 2 in the Modulation of the Estrogen Response of *pS2/TFF1* Gene

Amandine Chatagnon¹, Esteban Ballestar², Manel Esteller², Robert Dante^{1*}

1 INSERM, U590, Lyon, France, **2** Cancer Epigenetics and Biology Programme (PEBC), Catalan Institute of Oncology (ICO-IDIBELL), L'Hospitalet de Llobregat, Barcelona, Spain

Abstract

Background: In human Estrogen Receptor α (ER α)-positive breast cancers, 5' end dense methylation of the estrogen-regulated *pS2/TFF1* gene correlates with its transcriptional inhibition. However, in some ER α -rich biopsies, *pS2* expression is observed despite the methylation of its TATA-box region. Herein, we investigated the methylation-dependent mechanism of *pS2* regulation.

Methodology/Principal Findings: We observed interplay between Methyl-CpG Binding Domain protein 2 (MBD2) transcriptional repressor and ER α transactivator: (i) the *pS2* gene is poised for transcription upon demethylation limited to the enhancer region containing the estrogen responsive element (ERE); (ii) MBD2-binding sites overlapped with the methylation status of the *pS2* 5' end; (iii) MBD2 depletion elevated *pS2* expression and ectopic expression of ER α partially overcame the inhibitory effect of MBD2 when the ERE is unmethylated. Furthermore, serial chromatin immunoprecipitation assays indicated that MBD2 and ER α could simultaneously occupy the same *pS2* DNA molecule; (iv) concomitant ectopic ER α expression and MBD2 depletion resulted in synergistic transcriptional stimulation, while the *pS2* promoter remains methylated.

Conclusions/Significance: MBD2 and ER α drive opposite effects on *pS2* expression, which are associated with specific steady state levels of histone H3 acetylation and methylation marks. Thus, epigenetic silencing of *pS2* could be dependent on balance of the relative intracellular concentrations of ER α and MBD2.

Citation: Chatagnon A, Ballestar E, Esteller M, Dante R (2010) A Role for Methyl-CpG Binding Domain Protein 2 in the Modulation of the Estrogen Response of *pS2/TFF1* Gene. PLoS ONE 5(3): e9665. doi:10.1371/journal.pone.0009665

Editor: Axel Imhof, Ludwig-Maximilians-Universität München, Germany

Received: February 2, 2010; **Accepted:** February 18, 2010; **Published:** March 12, 2010

Copyright: © 2010 Chatagnon et al. This is an open-access article distributed under the terms of the Creative Commons Attribution License, which permits unrestricted use, distribution, and reproduction in any medium, provided the original author and source are credited.

Funding: The present work was supported by the Ligue Nationale contre le Cancer (Comite du Rhone and Comite de la Loire), the Institut National contre le Cancer (EpiPro and CircBio). The funders had no role in study design, data collection and analysis, decision to publish, or preparation of the manuscript.

Competing Interests: The authors have declared that no competing interests exist.

* E-mail: dante@univ-lyon1.f

Introduction

Global loss of DNA methylation and localized CpG island hypermethylation is a common characteristic of cancer cells [1–3], leading respectively to aberrant ectopic gene activation or inversely to gene silencing. The *pS2* gene (also called *TFF1*) has been identified by differential screening of a cDNA library from the human breast cancer cell line MCF7 [4]. In this cell line, its transcription is directly controlled by estrogens [5] and an estrogen responsive element (ERE) has been identified at nt positions –405 to –393, from transcription start site [5]. In breast tumors, expression of the *pS2* gene is correlated with the presence of estrogen receptors (ER), and it had been suggested that *pS2* expression increases cell proliferation and tumor cell survival [6,7]. Analysis of breast cancer biopsies or microdissected cells from formalin-fixed breast tissues has shown that *pS2* is hypomethylated in sub-classes of breast cancers [8,9].

We have previously shown [8] that the hypomethylation of the CCGG site close to the *pS2* ERE correlates with its expression in human breast cancer biopsies. Southern blots performed with methylation sensitive enzymes and bisulphite sequencing have indicated that the breast tumors analyzed exhibited different DNA methylation patterns at the 5' end of *pS2* [8]. Biopsies can display

either methylated, unmethylated and partially methylated 5' end *pS2* sequences at CpGs analyzed (nt positions –84 to +16) [8]. These observations prompted us to investigate the methylation-linked mechanisms of *pS2* gene repression and the potential involvement of DNA methylation in its response to estrogen stimulation.

In mammals, mechanisms implicated in the generation of a repressive state of chromatin associated with methylated DNA sequences have been investigated for over 20 years [10–13]. Pioneering studies led to the discovery of the Methyl-CpG binding domain (MBD) proteins family [14], which mediate DNA methylation-dependent gene silencing. The five *bona fide* MBD proteins, MeCP2, MBD1, MBD2, MBD3, and MBD4, share a canonical MBD. Biochemical and genetic analyses of these proteins have provided evidence of a direct link between DNA methylation and repressive chromatin architecture. MeCP2, MBD1 and MBD2 proteins bind to methylated DNA and recruit different histone deacetylase (HDAC)- and histone methyltransferase (HMT)-containing complexes that control chromatin compaction and gene silencing [15–17]. Mammalian MBD3, which lacks a functional MBD, does not recognize methylated DNA but is part of the histone deacetylase and chromatin remodeling Mi2/NuRD complex [18–20]. The last member of

this protein family, MBD4, is a thymine glycosylase primarily involved in DNA repair [21].

The involvement of MBD proteins in gene imprinting [22], X inactivation [23], and transcriptional silencing of genes possessing hypermethylated CpG islands in cancer cells [2,3] is now well documented. However, in contrast to the situation observed for DNMT-deficient mice, which either fail to develop or else die shortly after birth [24], the loss of MBD proteins, with the exception of MBD3, does not result in dramatic phenotypes [17], suggesting that MBD proteins deficiency causes subtle gene-expression changes.

Although the involvement of MBD proteins in gene silencing is well established, new facets regarding the links between DNA methylation, MBD proteins and gene transcription are emerging. For instance, it has been reported that DNA methylation in the body of genes can alter chromatin structure and reduce transcriptional elongation [25]. In parallel with the above findings, we have shown that the association of MBD2 with a methylated CpG island located downstream of the promoter region reduces the transcription of *NBR2* gene [26].

The density of methylation seems to be an important parameter in the MBD proteins-dependent repression. Several years ago, using *in vitro* methylated plasmids, it had been shown that the density of methylated CpG and promoter strength modulate transcriptional repression mediated by MeCP1 complexes containing MBD2 [27]. Furthermore, analysis of the transcriptional activity of patch-methylated plasmids microinjected into *Xenopus* oocytes has suggested a competition between transactivators and MBD proteins for the establishment of an open conformation [28]. All together, these data suggest that transcriptional repression mediated by DNA methylation is a consequence of a cross-talk between methylated CpG density, MBD proteins and transactivators.

To further explore the relative roles of methylated CpG patterns and the competition between transactivators and MBD proteins to influence or modulate gene transcription, we here investigate the expression of the estrogen-regulated *pS2/TFF1* (*Trefoil Factor 1*) gene [29] in cell lines exhibiting different DNA methylation patterns at its 5' end, unmethylated, regionally methylated, and fully methylated. In these cell lines, it was possible to manipulate artificially the Estrogen Receptor- α (ER α), the natural transactivator of *pS2*, and MBD protein levels, and therefore, use them to determine the contribution of these proteins to *pS2* expression.

Results

Correlation between methylation patterns and *pS2* transcriptional repression

Expression of *pS2* is driven by a complex promoter containing a promoter/enhancer region responsive to estrogens, EGF, a phorbol ester tumor promoter, c-Ha-ras oncoprotein, and c-jun protein [33]. Specifically, the 5' end of *pS2* possesses an estrogen-responsive element (ERE), conferring potential estrogen inducibility. In the ER α -rich MCF7 cell line, it has been shown [34] that proteins present on the *pS2* promoter in the absence of estradiol (E₂) include basal transcriptional factors, active polymerase II, certain HATs and HMTs. This basal transcriptional activity implies steroid-independent expression of *pS2*. Moreover, the 5' end of *pS2* (nt positions -464 to +314) is included in a CpG-poor region, G + C = 0.54%, CpG observed / CpG expected = 0.35. A correlation between the methylation status of the *pS2* promoter region and its expression has been observed in human tissues and the breast cancer cell lines [8,35]. Experimental evidences are also in favour of a role of DNA methylation in the repression of

pS2 transcription. In the ER α -rich MCF7 cells, *pS2* is unmethylated and transcriptionally active while in the ER α -negative MDA MB231 cell line the 5' end of *pS2* (nt positions -665 to +17) is fully methylated and the *pS2* gene is silenced, [35]. We have extended this analysis to the down stream region of *pS2* promoter, since it had been suggested that DNA methylation of the regions adjacent to a promoter region may affect transcription [26,36,37].

The methylation status of the 5' end of *pS2*, from nt positions -464 to +294, was investigated in MCF7 cells expressing *pS2* at a high level and MDA MB231 a *pS2* negative cell line (Figure 1A). Bisulphite conversion of DNA and sequencing of cloned PCR fragments, indicated that this region is unmethylated in MCF7 and fully methylated in MDA MB231 cells (Figure 1B). A screening failed to detect a human breast cancer cell lines exhibiting intermediate methylation patterns similar to that observed in breast cancer biopsies by Southern blot experiments

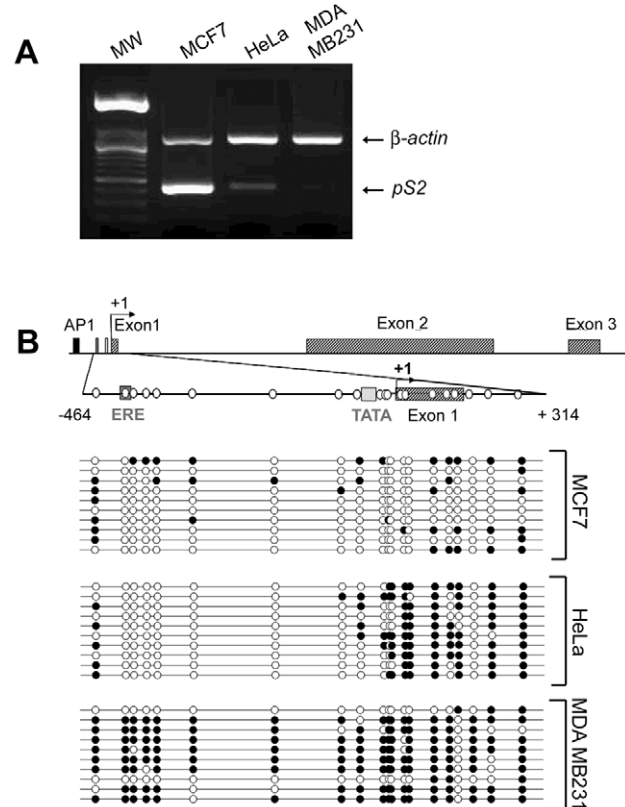


Figure 1. *pS2* gene expression and DNA methylation patterns in MCF7, HeLa and MDA MB231 cells. (A) The expression of endogenous *pS2* gene in MCF7, HeLa and MDA MB231 cell lines. *pS2* mRNA levels were monitored by relative RT-PCR. Briefly, *pS2* transcripts were simultaneously amplified with β -actin transcripts as a loading control and expression standard. (B) Methylation patterns at CpG sites of *pS2* 5' flanking sequence from nt positions -464 to +314 in MCF7, HeLa, and MDA MB231 cell lines. A schematic representation of the human *pS2* gene is shown. The transcription start site is indicated by a black arrow. Black box, AP1 site; dark-grey box, Estrogen-Responsive Element (ERE); light-grey box, TATA-box; hatched boxes, *pS2* exons. The studied region (from nt positions -464 to +314) is presented on an expanded scale. This region contains 20 CpG sites, represented by white circles. The bisulphite-sequencing status of this 5' *pS2* region in MCF7, HeLa and MDA MB231 cells (number of analyzed clones, n=10) is represented. Each line corresponds to a single DNA template molecule. Black and open circles represent methylated and unmethylated CpGs, respectively. doi:10.1371/journal.pone.0009665.g001

[8]. Nevertheless, some of these patterns, associated with low level of *pS2* transcripts (Figure 1A), are very similar to that observed in HeLa cells [8]. Thus, these cells were chosen for further analysis. HeLa cells exhibit an intermediate DNA methylation pattern, the CpGs spanning the -464 to -84 region, which includes the ERE are unmethylated, while the TATA-box region is methylated (Figure 1B). These data confirm the inverse correlation between *pS2* expression and the density of the methylation of its 5' end, suggesting that the methylation patterns around the transcription start site impact in the activity of *pS2* promoter in these cells.

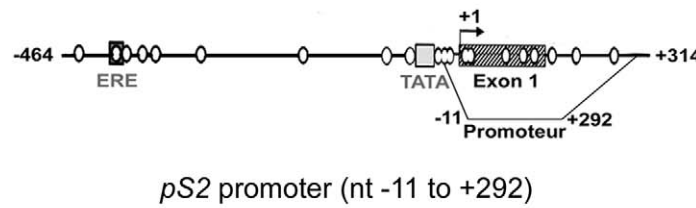
Specific binding of MBD2 to the methylated *pS2* promoter

Among the proteins involved in the methylation-dependent repression of transcription, MBD proteins seem to play a major role. Therefore, we assessed the presence of MBD proteins on *pS2*

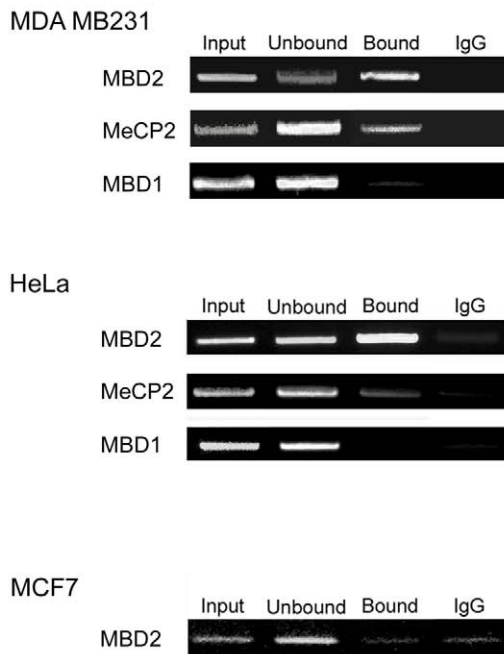
promoter by chromatin immunoprecipitation (ChIP) assays using antibodies directed against MBD1, MBD2 and MeCP2.

Representative experiments from at least three independent assays for each antibody are shown in Figure 2A. As a control, the fractions immunoprecipitated with a non-MBD protein-specific antibody (anti-mouse IgG) were also analyzed. In order to determine *pS2* DNA fragment enrichment in MBD immunoprecipitated fractions, a dose-dependent and quantitative (Q-PCR) amplifications (Figure 2A, B) using an equal quantity of DNA (0.5 ng) per PCR assay, were performed with each fraction obtained from the ChIP procedure. We focused this analysis on the *pS2* methylated promoter region, shared by HeLa and MDA MB231 cells (nt positions -11 to +292).

In the *pS2*-methylated cells, MDA MB231 and HeLa, when antibodies against MBD2 were used, the amount of *pS2* promoter per ng of total DNA in immunoprecipitated fraction (Figure 2A,



A



B

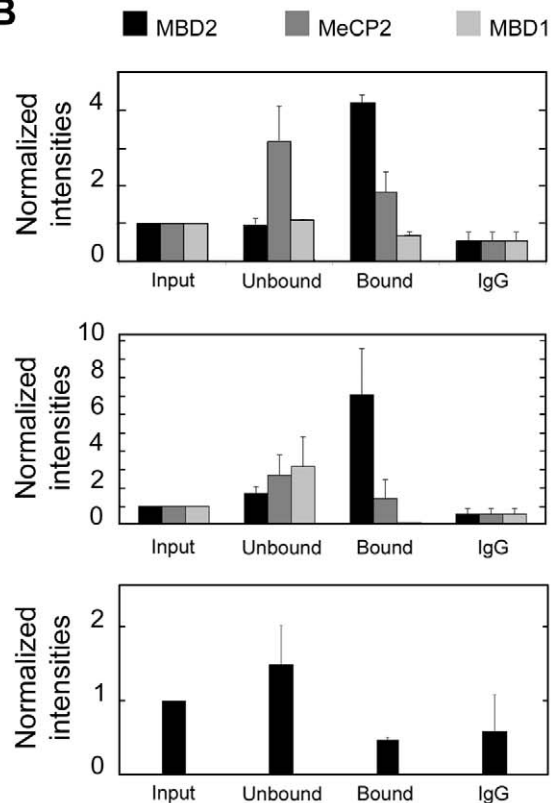


Figure 2. Specific association of MBD2 to the methylated promoter region of *pS2* gene. Detail of the *pS2* gene region analyzed (from nt positions -464 to +314). CpG sites are represented by circles. The black line represents the position of the fragment amplified by dose-dependent and quantitative PCR after ChIP. MBD proteins binding to the methylated region of the *pS2* promoter (from nt positions -11 to +292) was analyzed by ChIP in MDA MB231, HeLa and MCF7 cells. Cross-linked chromatin was immunoprecipitated using rabbit polyclonal anti-MBD2, anti-MeCP2 and anti-MBD1 antibodies. Purified DNAs from the input, unbound, bound or IgG fractions were quantified and an equal quantity of each fraction (0.5 ng) of this DNA was amplified by dose-dependent (A) or quantitative (B) PCR. (A) Representative experiments of MBD occupancy in the *pS2* promoter are shown. (B) Relative amounts of immunoprecipitated *pS2* promoter to the input fraction measured by quantitative PCR. Each bar represents the mean \pm standard deviation of at least three independent experiments. doi:10.1371/journal.pone.0009665.g002

“bound”) was greater than in the input, or in the non-retained fractions (Figure 2A, “input”, “unbound”, and “IgG”), indicating that this methylated region is immunoprecipitated by anti-MBD2 antibodies. In contrast, ChIP assays with anti-MeCP2 or anti-MBD1 antibodies led to a depletion of this DNA segment in the bound fractions (Figure 2A). Western blot analysis, using antibodies directed against MeCP2 and MBD1, produced a signal of the expected sizes [14], ~85 kDa and ~70 kDa, respectively (data not shown), indicating that both proteins are expressed in MDA MB231 and HeLa cells. As an additional control of MBD2-ChIP assays, we also amplified the -11 to +292 *pS2* region from MCF7-chromatin immunoprecipitated by anti-MBD2 antibodies (Figure 2A). As expected, no enrichment was observed in the bound fraction, since this region was unmethylated in the MCF7 cell line (Figure 2A). Taken together, these data strongly suggest that MBD2 binds selectively and specifically the methylated region of this promoter.

High resolution MBD2 binding profiles analysis of *pS2* promoter indicates that MBD2 specifically binds the methylated *pS2* promoter region and does not spread to the unmethylated ERE in HeLa cells

In HeLa cells, the bimodal methylation status of the *pS2* 5' end suggests that only some regions would actually be bound by MBD2. The unmethylated region containing the ERE (nt positions -405 to -393) is very close to the methylated TATA-box region (beginning at nt -9). ChIP experiments are not appropriate to discriminate between these two regions, as they are below the limit of resolution of the assay. Standard sonication of

crosslinked chromatin leads to 300–500 bp DNA fragments and attempts to reduce its length (100–200 bp) resulted in a loss of efficiency in immunoprecipitation. Therefore, to precisely map the MBD2 binding sites we used a high-resolution method based on a ChIP-on-chip approach (Chatagnon *et al.*, manuscript in preparation). DNAs obtained from HeLa cell chromatin immunoprecipitated by anti-MBD2 antibodies were hybridized on an Affymetrix Human Promoter 1.0R Array (ChIP-on-chip).

ChIP-on-chip experiments indicated that MBD2 associated specifically the region containing the methylated *pS2* TATA-box, where a strong positive signal (red bars) is observed, while the region containing the unmethylated ERE is devoid of MBD2. Thus, the positive signals for MBD2 binding parallels the methylation status of the *pS2* 5' end and indicates that MBD2 does not spread outside the methylated region on *pS2* promoter (Figure 3A). As a control, results obtained for a previously identified MBD2 free promoter [26], *BRCA1*, are also shown on Figure 3B. Consistent with previous findings, no MBD2 positive signal was observed in the region spanning the nucleotides -1000 to +1000 of *BRCA1* (Figure 3B).

MBD2 acts as a methylation-dependant transcriptional repressor of *pS2* transcription

The correlation between levels of *pS2* expression and the presence of MBD2 in the TATA-box region argues in favour of a repressive effect of MBD2 on *pS2* transcription. To examine this further, we depleted cells from MBD2 by transient transfection of siRNA targeted *MBD2* transcripts. Quantitative competitive RT-PCR assays indicated a significant reduction of the *MBD2* mRNA

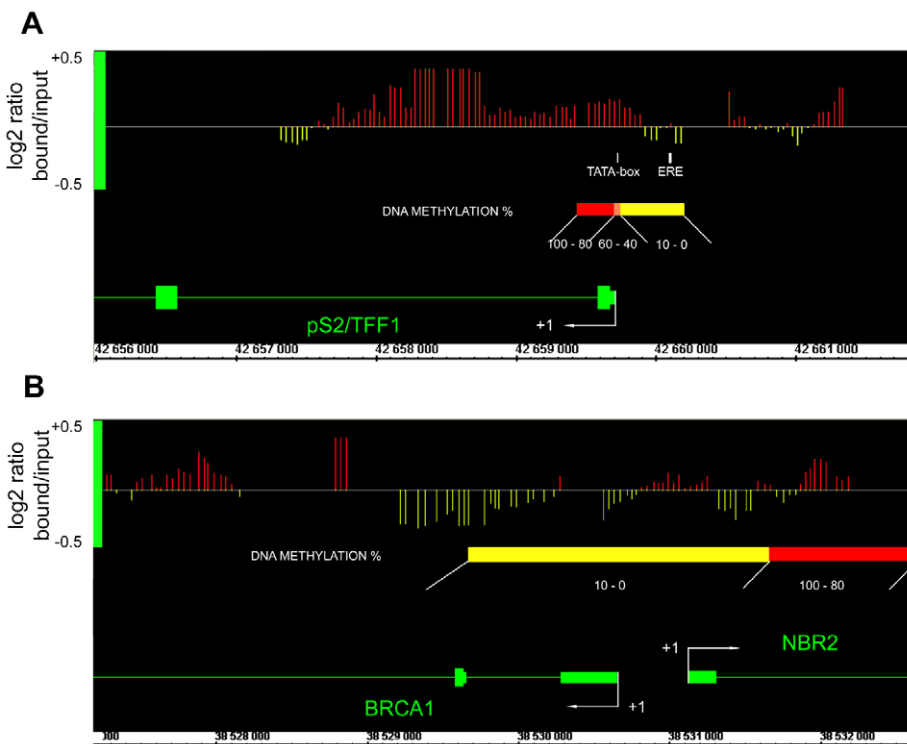


Figure 3. ChIP-on-chip analysis of MBD2-binding sites on *pS2* 5' end regionally methylated in HeLa cells. (A) Array peaks on *pS2* 5' end of MBD2 log₂ signal ratio (MBD2 / Input) values are shown below the Affymetrix' Integrated Genome Browser (IGB) window. Red bars, MBD2 binding sites; yellow bars, MBD2 free sites. Genes are transcribed from right to left. *pS2* methylation status from nt positions -464 to +314 is shown by a diagram. “*pS2* ERE fragment” and “*pS2* promoter fragment” analyzed by PCR following ChIP are represented by a white box. **(B)** *BRCA1* 5' end viewed as a MBD2 free control.

doi:10.1371/journal.pone.0009665.g003

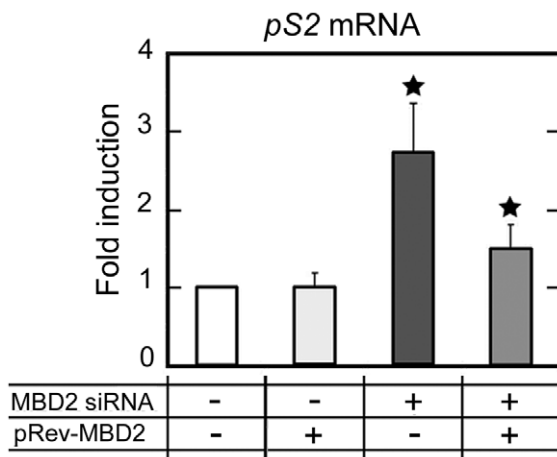


Figure 4. MBD2 specifically and directly represses *pS2* transcription. Real time RT-PCR analysis of *pS2* transcripts in HeLa and MBD2-depleted HeLa cells (HeLa cells pretreated for 72 h with MBD2 siRNA) transfected with an MBD2 vector expressing a transcript resistant to RNAi (pRev-MBD2 vector) or with an empty basic vector pGL3. Transcriptional expression of *pS2* was analyzed 24 h after transfection. The fold change of *pS2* expression was calculated from the relative *pS2* mRNA in pRev-MBD2-transfected cells compared to pGL3-transfected cells. Values are presented as the mean \pm standard deviation of at least three independent transfection experiments. A significant difference between the two cell groups is represented by an asterisk * ($P < 0.05$). doi:10.1371/journal.pone.0009665.g004

level (by 87–93%) (Supplemental Figure S1A). Moreover, in HeLa cells, western blot analysis also revealed a dramatically lower abundance of MBD2 proteins in the MBD2 siRNA-treated cells compared with control cells (Supplemental Figure S1B). Furthermore, the expression of MeCP2 and MBD1 was not different in MBD2 knockdown HeLa cells than in wild-type or mock-treated cells (Supplemental Figure S1B).

In the *pS2*-fully methylated cells MDA MB231, MBD2 depletion (about 90%), did not induce *pS2* expression (Supplemental Figure S1C). However, in MBD2 siRNA-treated HeLa cells, *pS2* expression is stimulated approximately 3-fold (Figure 4), while the methylation level of *pS2* TATA box region and ER α expression remain unaffected (data not shown). In MBD2 siRNA-treated HeLa cells, transient expression of an *Mbd2* cDNA, refractory to siRNA-mediated decay [26], shifted down the *pS2* mRNA level (Figure 4). Additional dose of Mbd2 in HeLa cells, containing normal levels of MBD2 proteins, did not affect *pS2* expression (Figure 4). Thus, the amount of MBD2 protein is not a limiting factor in the transcriptional repression of *pS2* in these cells. In MCF7 cells, quantitative RT-PCR showed that the level of *pS2* expression is unaffected by MBD2 depletion, indicating that MBD2 siRNA did not elevate *pS2* expression by an off-target effect since *pS2* is not bound by MBD2 in these cells (Supplemental Figure S1C).

ER α only bound *pS2* ERE when unmethylated in cell lines

To determine whether ER α can be recruited on the *pS2* ERE sequence when this region or the adjacent region is methylated, we artificially manipulated the level of ER α in MDA MB231 and HeLa cells, which are deficient in this protein.

ChIP assays, using anti-ER α antibodies, were performed from HeLa and MDA MB231 cells transiently transfected with the vector HEG0 encoding ER α . ER α -rich MCF7 cells were used as a positive control and untransfected HeLa and MDA MB231 cells as negative controls. As expected, ChIP assays performed from MCF7 chromatin indicated that the amount of *pS2* DNA per ng of total DNA in immunoprecipitated fraction (Figure 5, “bound”) is higher (about 8-fold, Q-PCR assays) than in input, or non-retained fractions (Figure 5, “input”, “unbound”, and “IgG”) while no enrichment in *pS2* sequence was observed in immunoprecipitated fraction obtained from untransfected HeLa and MDA MB231 cells (Figure 5). All together, these data indicate that anti-ER α antibodies specifically precipitated chromatin bound by ER α .

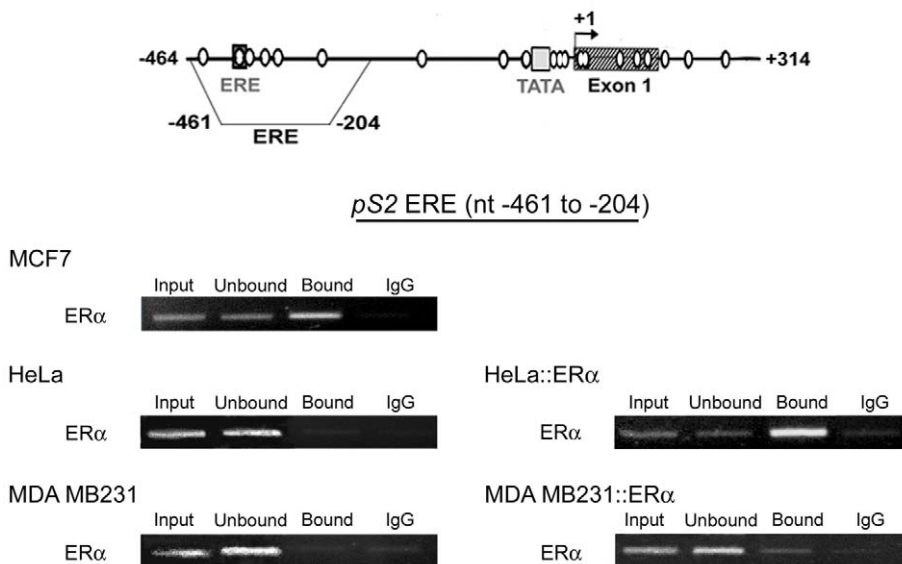


Figure 5. ER α only associates hypomethylated ERE region of *pS2*. Representative experiments of ER α ChIP assays in ER α -rich MCF7 cells, in ER α -negative HeLa and MDA MB231 cells, and in HeLa and MDA MB231 expressing the vector HEG0 encoding ER α (HeLa::ER α , and MDA MB231::ER α). ChIP assays were performed as described in Figure 2. The position of the “*pS2* ERE fragment” analyzed by PCR are represented on the *pS2* 5’ end schema. doi:10.1371/journal.pone.0009665.g005

In HeLa cells, transient expression of the vector HEG0 coding for ER α , leads to enrichment in *pS2* sequence in the immunoprecipitated fraction (Figure 5). This enrichment (about 10 fold, Q-PCR assays) was comparable to that observed in MCF7 cells, indicating that ER α is efficiently recruited on the *pS2* ERE site in HeLa cells. In contrast, in MDA MB231 cells, despite ectopic expression of ER α , *pS2* sequence was not selectively immunoprecipitated by the anti-ER α antibodies (Figure 5). Thus, ER α does not bind the methylated *pS2* ERE in MDA MB231 cells, suggesting that full DNA methylation induces chromatin changes that prevent ER α binding.

Ectopic expression of ER α enhances *pS2* gene expression only when its 5' end region is partially methylated, in ER α negative cells

The ERE of the *pS2* promoter can act as a strong enhancer in the presence of E₂ and ER α [29,33]. To analyze the potential antagonistic activity of MBD2 and ER α on *pS2*, ectopic expression of ER α was induced in MDA MB231 and HeLa cells.

Transient expression of ER α elevated *pS2* expression by a 4-fold (Figure 6), in HeLa cells. This stimulation by ER α of *pS2* transcription did not affect the methylation status of HeLa *pS2* promoter (data not shown). ER α stimulation of *pS2* expression was fully reversed by antiestrogen (4-hydroxytamoxifen, OHT) treatments (Figure 6), while the basal level of *pS2* expression was conserved. These results indicate the existence of estrogen-dependent transactivation of *pS2* in HeLa cells. As expected, *pS2* expression was not induced in MDA MB231 cells (data not shown), since ER α did not bound *pS2*-ERE sequence in this cell line (Figure 5). These results suggest that demethylation of ERE region allows the estrogen response of *pS2* in HeLa cells.

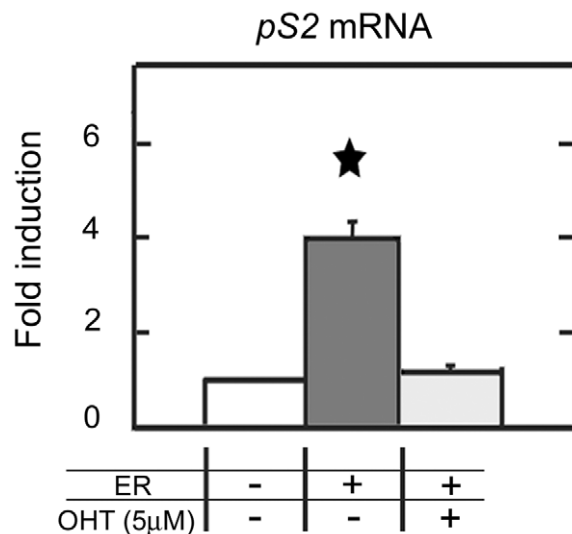


Figure 6. ER α stimulates *pS2* transcription in HeLa cells. Real time PCR quantification of *pS2* mRNA in HeLa cells ectopically expressing ER α . HeLa cells were transfected with the vector HEG0 coding for ER α and *pS2* expression was monitored 24h after. To investigate the estrogen dependence of *pS2* expression, cells were exposed to 5 μ M of antiestrogen (4-hydroxytamoxifen or OHT). Bar chart show the fold change of *pS2* expression calculated from the relative *pS2* mRNA in HEG0-transfected cells compared to pSG5, empty vector-transfected cells. Each bar represents the mean \pm standard deviation of three analyses. A significant difference between the two cell groups is represented by an asterisk * ($P < 0.05$). doi:10.1371/journal.pone.0009665.g006

MBD2 is not displaced from the *pS2*-methylated promoter region by ER α transactivation, in HeLa cells

HeLa cells expressing the vector encoding ER α were used to identify the proteins bound to the 5' end of *pS2*. Dose-dependent and quantitative PCR amplifications of each fraction obtained from the ChIP procedure were performed. These assays showed that MBD2 was still present on the methylated region of *pS2* promoter (Figure 7A), and the enrichment in the bound fraction was not modified by the presence of ER α on the ERE (Figure 7A). These results provide evidence that ER α can overcome, at least partially, the inhibitory effect of MBD2 binding to *pS2* promoter and imply that both proteins can occupy the 5' end of the *pS2* gene.

To address this matter, we performed serial ChIP assays. A first round of immunoprecipitation was carried out with an anti-ER α antibody from HeLa cells transiently transfected with the vector HEG0 encoding ER α . Then, immunoprecipitated cross-linked DNA-protein complexes were isolated and subjected to reimmunoprecipitation using antibodies directed against MBD2. PCR amplification of *pS2* promoter region from the fraction reimmunoprecipitated with anti-MBD2 antibodies gave a positive signal

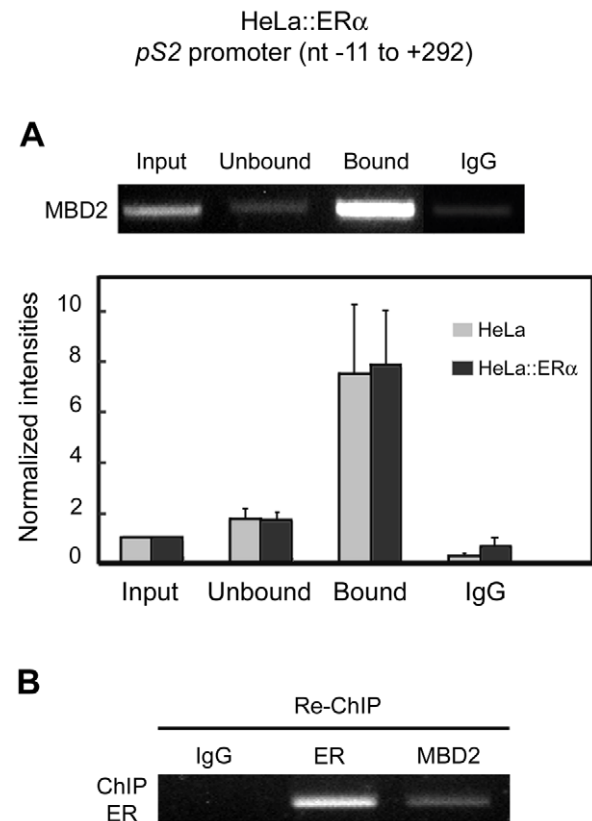


Figure 7. The transactivators ER α and the methylation-dependant repressor MBD2 can simultaneously bound the *pS2* promoter in HeLa cells. (A) MBD2 ChIP assays in HeLa cells expressing ER α (HeLa:ER α). Relative amounts of immunoprecipitated *pS2* promoter measured by quantitative PCR from HeLa or HeLa:ER α cells. Each bar represents the mean \pm standard deviation of at least three independent experiments. (B) Serial ER α -MBD2 ChIP assays to *pS2* promoter. Chromatin prepared from HeLa cells transfected with a human ER α expression vector was subjected to the ChIP procedure with the anti-ER α antibody, and again immunoprecipitated using antibodies as indicated at the top of the figure (Non-specific antibody, IgG; anti-ER α antibody, ER; anti-MBD2 antibody, MBD2). doi:10.1371/journal.pone.0009665.g007

(Figure 7B). In control reactions, as expected, no signal was detected with non-specific antibodies, while a positive signal was observed in the fraction reimmunoprecipitated with anti-ER α antibodies (Figure 7B). Thus, the binding of ER α on the ERE of *pS2* does not displace MBD2 from the methylated TATA-box region, since both proteins were present on the same DNA molecules.

Synergic activity of MBD2 depletion and ectopic ER α expression on *pS2* transcription, in HeLa cells

The opposite effects of MBD2 and ER α proteins on *pS2* expression suggest an antagonistic action between these two transcriptional regulators, in HeLa cells. To investigate this possibility, the concentrations of MBD2 and ER α proteins were artificially manipulated in these cells. After MBD2 depletion mediated by RNA interference, ectopic ER α expression resulted in a dramatic (approximately 31-fold) enhancement of *pS2* mRNA concentration, approaching the level to that observed in MCF7 (Figure 8A, B). Thus, *pS2* responses to ER α activation (4-fold increase) and MBD2 depletion (3-fold increase) are not additive and suggest a cross-talk between these two transcriptional regulators. Concomitant exposure to OHT knocked down *pS2* expression to the level observed in HeLa cells transfected by MBD2 siRNA alone, (about 3-fold) when compared with control HeLa cells (Figure 8A, B). It should be noted that *pS2* transcription cannot be induced by concomitant ectopic expression of ER α and MBD2 depletion when its 5' end is fully methylated, as observed in MDA MB231 cells (data not shown). In cells exhibiting a bimodal methylation profile as HeLa cells, a synergic activation was observed. Thus, the binding of MBD2 to the methylated TATA-box of *pS2* reduces but does not abolish *pS2* response to ER α , suggesting that as a result of regional demethylation, *pS2* is poised for transcription.

Post-translational modifications of histone H3 are associated with *pS2* expression induction

To get further insight on the mechanism involved in the opposite effect of MBD2 and ER α on *pS2* transcription, we investigated histone modifications in HeLa cells. It is well known that both proteins, MBD2 and ER α , regulate the transcription by the recruitment of chromatin remodeling complexes [15,38]. Importantly, ER α has been shown to interact with several coactivators with histone acetyltransferase activity (CBP, p300, p/CAF and the members of p160 family) [38], or histone demethylase (LSD1) [39]. Conversely, MBD2 recruits corepressors with histone deacetylase activity (Mi2/NurD) [17]. Histone H3 acetylation (H3Ac) and histone H3 lysine 9 (H3K9) trimethylation chromatin marks have been the subject of intense investigation during the past few years and appear to be associated with active and silent promoters, respectively.

In our study, ChIP assays indicated that ER α *pS2* stimulation was associated with increase in histone H3 acetylation (~2.5 fold) and enhanced the demethylation of H3K9 (~500 fold) at *pS2* promoter, when compared with wild type HeLa cells (Figure 9). Moreover, in HeLa cells, the synergic activity of MBD2 depletion and ectopic ER α expression on *pS2* transcription led to a stronger induction of histone H3 acetylation (~28 fold) at *pS2* promoter, while H3K9 methylation was still lowered (~10 fold), (Figure 9). From these findings we conclude that the transcriptional MBD2 repressor and ER α transactivator co-participate to the regulation of *pS2* expression by mediating a balance between repressive histone H3 lysine 9 trimethylation and active histone H3 acetylation marks at *pS2* promoter. Thus, the repressive effect of

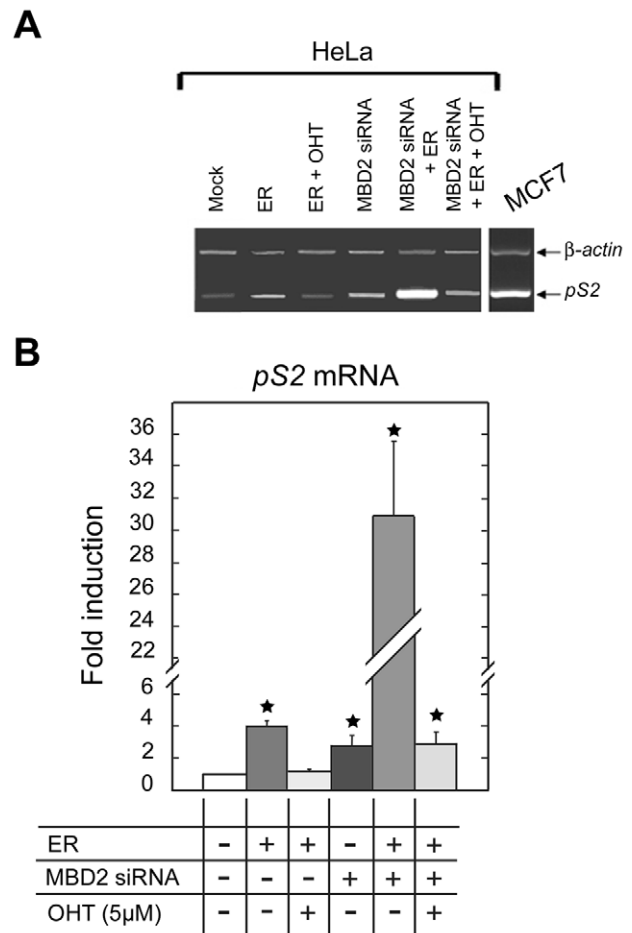


Figure 8. MBD2 modulates the estrogen response of *pS2* gene. (A) Transcriptional expression of *pS2* was analyzed using relative RT-PCR in HeLa cells expressing ER α and/or depleted in MBD2. Mock, mock-treated HeLa cells. ER, HeLa cells 24 h after transfection with a human ER α expression vector, HEG0. MBD2 siRNA, HeLa cells pretreated for 72 h with MBD2 siRNA and again for 24 h. MBD2 siRNA + ER, HeLa cells pretreated for 72 h with MBD2 siRNA, then cotransfected with MBD2 siRNA and HEG0 for 24 h. OHT, 24 h treatment with 4-hydroxytamoxifen. MCF7, MCF7 cells. (B) Bar chart showing the fold change of *pS2* expression in HeLa cells expressing ER α and/or depleted in MBD2. *pS2* transcripts were quantified by real time RT-PCR. The fold change was calculated from the relative *pS2* mRNA in treated compared to mock-treated cells. Each bar represents the mean \pm standard deviation of three analyses. A significant difference between the two cell groups is represented by an asterisk * ($P < 0.05$). doi:10.1371/journal.pone.0009665.g008

MBD2 on the transactivation of *pS2* mediated by ER α is linked to histone modifications.

Discussion

In cancer tissues and cell lines, transcriptional silencing associated with aberrant methylation of promoter regions is now regarded as an almost universal epigenetic marker of malignant transformation [1–3]. Since the first experiments showing that the MBD2 binds *in vivo* to the methylated regulatory regions of *p16* and *p14* and could thereby contribute to gene silencing in colon carcinoma cell lines [40], a body of evidence has accumulated concerning associations between MBD proteins and hypermethylated promoter regions [41–43]. In non-pathological situations, MBD proteins are also directly involved in the repression of

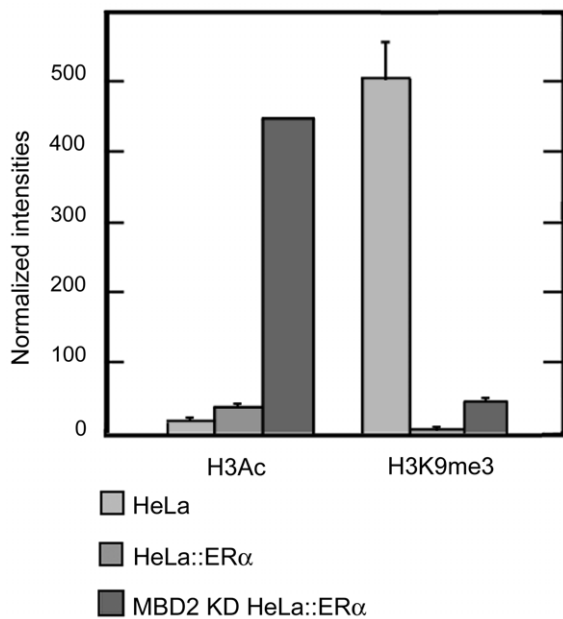


Figure 9. Histone H3 marks on *pS2* promoter in presence or absence of MBD2 and/or ER α . HeLa cells, wild type (HeLa), expressing ectopically ER α (HeLa::ER α), and depleted in MBD2 and expressing ectopically ER α (MBD2 KD HeLa::ER α), were subjected to ChIP analysis using anti-histone H3 acetylation (H3Ac) or an anti-histone H3 lysine 9 trimethylation (H3K9me3) antibodies. The *pS2* promoter was amplified by real-time PCR from an equal amount (0,5 ng) of total DNA immunoprecipitated by the different antibodies. Relative amounts of H3Ac or H3K9me3 marks were measured by comparing fractions immunoprecipitated by the anti-H3Ac or anti-H3K9me3 antibodies to fractions immunoprecipitated by the anti-histone H3 pan antibody. Each bar represents the mean \pm standard deviation. doi:10.1371/journal.pone.0009665.g009

imprinted genes and differentiation-dependent gene expression [17].

In unmethylated MCF7, methylated MDA MB231, and regionally methylated HeLa cells, we found that MBD2 binding profiles parallel the methylation patterns of the *pS2* 5' end, while MeCP2 and MBD1 were not detected in this region. Furthermore in HeLa cells, high resolution mapping of MBD2 binding sites indicated that MBD2 only associated the methylated region close to the TATA-box, whereas the unmethylated region, including the *pS2* ERE, was not targeted by this repressor.

MBD2 depletion by siRNA targeting *MBD2* transcripts elevated *pS2* transcription by a factor of ~ 3 in HeLa cells, while, in unmethylated cells (MCF7), *pS2* expression was not affected by MBD2-specific siRNA transfection suggesting a direct relationship between *pS2* repression and MBD2 binding.

Injection in *Xenopus laevis* oocytes of regionally methylated plasmids has shown that a few methylated cytosines can inhibit a flanking promoter but a threshold of modified sites is required to organize a stable, diffusible chromatin structure. From these data and results obtained with chemical inhibitor of histone deacetylase, these authors have proposed that a specialized chromatin structure, formed not only by MBD proteins but also by other structural and remodelling activities, is organized on the modified DNA, when the number of methylated sites is increased and reaches the threshold that leads to diffusion of gene silencing on the DNA fiber [28]. In agreement with this hypothesis, MBD2 depletion did not induce *pS2* transcription in MDA MB231 cells exhibiting fully methylated *pS2* 5' end.

The present study also indicates that ER α only associates the unmethylated *pS2* ERE independently of the methylation status of the TATA-box region, since the same level of ER α was observed at the ERE region in MCF7 cells and in HeLa cells transiently transfected with the HEG0 vector encoding this receptor. In contrast, strong expression of ER α upon transient transfection with HEG0, did not lead to ER α binding in MDA MB231 cells, suggesting that full methylation of the 5' end of *pS2* prevents its binding. Although a direct effect cannot be totally excluded, we have previously shown, using electrophoretic mobility assays, that methylated oligonucleotides containing the *pS2* ERE are efficiently recognized by ER α [44]. *In vivo* experiments also suggest an indirect effect of DNA methylation. In the HE5 cell line derived from MDA MB231 that expresses functional ER α , but not *pS2*, DNase I hypersensitive sites are not modified by ER α expression, while in the ER α and *pS2* positive MCF7 cells display hormone-dependent hypersensitive DNase sites at the *pS2* ERE region [45]. Thus, the methylation of TATA-box region does not seem to lead to diffusible alteration of chromatin structure, in HeLa cells.

As expected from the analysis of methylation and ER α binding sites profiles, ectopic expression of ER α in MDA MB231 cells did not stimulate *pS2* expression. In HeLa cells, ER α induction of *pS2* expression was observed suggesting that the demethylation of ERE region seems to be a prerequisite for estrogen-dependent *pS2* stimulation. Nevertheless, the level of *pS2* transcript remained relatively low when compared with that observed in E₂ treated MCF7 cells. The present study indicates that high levels of ER α can at least partially overcome the transcriptional repression mediated by MBD2 without affecting the methylation status of the *pS2* promoter. Thus, the binding of MBD2 to the methylated TATA-box of *pS2* reduces but does not abolish *pS2* response to ER α .

The mapping of MBD2 binding sites at *pS2* locus indicated that MBD2 proteins lay downstream the initiation start site. The analysis of the 5' region of the endothelin receptor B gene in human cell lines shows that extensive methylation closely downstream of the initiation site does not abolish gene expression [46]. However, the impact of intragenic methylation has been studied from transgenes methylated exclusively in a region downstream of the promoter, into a specific genomic site. This methylation pattern induces a close chromatin conformation and decrease transcription levels, suggesting that this epigenetic mark may reduce the efficiency RNA polymerase II elongation [25]. Thus, we cannot exclude that DNA methylation and MBD2 binding downstream *pS2* promoter region may impact elongation rate. However, we observed post-translational modifications of histone H3 (acetylation and demethylation) at the promoter region, when *pS2* transcription is induced by MBD2 siRNA and/or ER α expression, suggesting that MBD2 depletion influences chromatin conformation at *pS2* promoter.

Recently, it has been published that, upon E₂ induction, synchronized human cell lines exhibit a cyclical methylation/demethylation of the *pS2* ERE region correlated with cyclical binding of transcriptional repressors/activators [47,48], when the 5' end of *pS2* is unmethylated [35,48]. Although the maintenance of DNA methylation patterns begin to be well described, it will also be important to consider mechanisms that enable the removal of these marks to fully comprehend the dynamic behavior of DNA methylation, as suggested by recent reports [47,48]. Nevertheless, the mechanisms and enzymatic activities that are responsible for DNA demethylation in mammals although potentially linked to DNA repair are controversial [47–53].

Transcriptional repression mediated by MBD proteins can be reversed by various mechanisms. In mouse and rat, Mecp2 is

directly involved in a depolarization-controlled repression of the *brain-derived neurotrophic factor (Bdnf)* gene in neurons [54,55]. This protein, associated with the corepressor Sin3a, binds to a CpG-poor methylated region of *Bdnf* promoters. Upon the initiation of Ca^{++} signaling, Mecp2 becomes phosphorylated and is liberated from the promoter as *Bdnf* is activated. Mbd2 is also able to repress CpG-poor methylated promoter. In Mbd2 null mice, ectopic expression of interleukin-4 (Il4) disrupts T-helper cell differentiation, suggesting that Mbd2 is a transcriptional repressor of Il4 in naïve T cells. Indeed, in naïve wild type T cells, overexpression of the transcription factor GATA-3, normally required for Il4 expression, displaces Mbd2 from the promoter and activates Il4 transcription [56].

The interplay between ER α and MBD2 in *pS2* transcription indicates that the partial reversion of transcriptional repression mediated by MBD2 does not necessarily involve the displacement of this repressor from its CpG-poor promoter region. In the model studied, the amounts of *pS2* gene immunoprecipitated by anti-MBD2 antibodies was not affected by the binding of ER α . In addition, serial ChIP assays showed that *pS2* promoter region can be simultaneously bound by ER α and MBD2 proteins. Furthermore, the synergic effects of ectopic ER α expression and depletion of MBD2 on *pS2* transcription also suggest that both proteins do not compete for *pS2* promoter occupancy.

Data, obtained from experiments performed on cell lines, indicate that methylation-dependent repression of *pS2* expression is mediated by MBD2. Nevertheless, ER α binding can counteract the inhibitory effect of DNA methylation without displacing MBD2 proteins from the TATA-box region. Taken together these data might explain *pS2* expression in some ER α -rich breast cancers despite the methylation of its TATA-box.

Materials and Methods

Cell culture

MDA MB231, MCF7, and HeLa cells were obtained from the American Type Culture Collection (ATCC, Rockville, MD). Cells were maintained in Dulbecco's modified Eagle's medium (DMEM) containing 1g/l glucose (Eagle, Sigma, L'isle d'Abeau, France) and supplemented with 10% of heat inactivated fetal bovine serum (Lonza, Vervier, Belgium) and grown at 37°C in a humidified 5% CO₂ atmosphere.

Due to the poor efficiency of repeated siRNA treatments associated with vector transfections in estradiol depleted medium by charcoal extraction, all the experiments were performed in standard DMEM medium supplemented with fetal bovine serum. To investigate the estrogen dependence of *pS2* expression, cells were exposed to estradiol or to 5 μ M 4-hydroxytamoxifen (OHT).

Sodium bisulphite modification

Sodium bisulphite reactions were carried out as previously described [30]. Two regions (nt positions -464 to +67, and nt positions +37 to +314 from the *pS2* transcription start site) within the *pS2* promoter gene were analyzed. PCR amplifications were accomplished in 100 μ l using the HotStart *Taq* DNA polymerase Kit (Qiagen, Courtaboeuf, France) and 0.25 μ M of the primers (Supplemental Table S1), after 15 min at 95°C for *Taq* polymerase activation and 35 cycles (30 s denaturation at 94°C, 1 min annealing at 52°C, and 1.5 min extension at 72°C). To determine accurately the proportion of methylated CpG, PCR products were cloned into a pGEM-T vector (Promega, Lyon, France) and 10 random clones from each sample were analyzed by automatic sequencing (Biofidal, Lyon, France).

Chromatin Immunoprecipitation (ChIP) assays

Nucleoprotein complexes were sonicated to reduce the length of DNA fragments to 300–600 bp, and ChIP assays were carried out as described previously [26]. Fifteen μ l of two different polyclonal anti-MBD2 antibodies (kindly provided by Dr. P. Wade and Dr. E. Ballestar) or 20 μ l of polyclonal anti-MBD1 (Abcam, Cambridge, UK), anti-MeCP2 (Upstate Biotechnology, Lake Placid, NY) antibodies, or 2.5 μ g of polyclonal anti-ER α antibody (Santa Cruz Biotechnology, Inc, Santa Cruz, CA) or anti-mouse IgG (Dakocytomation, Trappes, France), were used for immunoprecipitation. DNA samples obtained from the input, unbound and bound fractions were quantified by densitometry using the VersaFluor™ Fluorometer (Biorad, Ivry, France) and RiboGreen reagent (Molecular Probes, Interchim, Montluçon, France). The amounts of DNA in IgG control fractions were at the limit of the fluorometric detection methods. Thus, PCR quantification of DNA fragments in IgG fractions was not accurate as in other fractions, since we have used very large parts of the “IgG fractions” when compared with the other fractions.

PCR assays were performed to assess the binding of the proteins to the *pS2* 5' flanking sequence. Two regions were analyzed: “*pS2* ERE fragment” (from nt positions -461 to -204 from the *pS2* transcription start site) and “*pS2* promoter fragment” (from nt positions -11 to +292). We amplified, by dose-dependent and quantitative PCR (Q-PCR), equal amounts of total DNA (0.5 ng) from the input, unbound and bound fractions. HotStar *Taq* polymerase kit (Qiagen) and 0.4 μ M of the primers (Supplemental Table S1) were used in classical PCR. After 15 min at 95°C for *Taq* polymerase activation and 37 cycles (30 s denaturation at 94°C, 1 min annealing at 53°C, and 1.5 min extension at 72°C) for the “*pS2* ERE fragment” or 36 cycles (30 s denaturation at 94°C, 1 min annealing at 58°C, and 1.5 min extension at 72°C) for the “*pS2* promoter fragment”, PCR products were analyzed on a 2% agarose gel containing 1 μ g/ml ethidium bromide and were quantified by densitometry. Real-time PCR was carried out using LightCycler® Fast Star DNA Master PLUS SYBR Green I System (Roche Molecular Biochemicals, Maylan, France) and 0.4 μ M of the primers (Supplemental Table S1). Cycling parameters were 95°C for 10 min followed 45 cycles at 95°C for 10 s, 64°C for 5 s and 72°C for 10s.

ChIP-on-chip

For ChIP-on-Chip analysis, the specific protein-DNA complexes were obtained from independent immunoprecipitations using two different polyclonal anti-MBD2 antibodies (kindly provided by Dr. P. Wade and Dr. E. Ballestar). The ChIP DNAs from the input and bound fractions were amplified, labelled and hybridized on microarrays by ProfileXpert service according to Affymetrix™ protocols. Briefly, the ChIP DNA was amplified by random PCR. Enrichment of MBD2-bound sites during the amplification procedure was assayed, by PCR amplification of *NBR2* [26] and *pS2* promoters, on each ChIP samples before and after amplification. The amplified DNAs were then labelled using the GeneChip® WT Double - Stranded DNA Terminal Labelling Kit and hybridized to the human tiling arrays (Human Promoter 1.0R Arrays), which were then washed and scanned. Raw data from the scans were analyzed using Affymetrix® Tiling Analysis Software (TAS) and the results were viewed in Affymetrix' Integrated Genome Browser (IGB) Software.

Serial ChIP assays (ChIP re-ChIP)

The ERE and the TATA box regions of *pS2* are placed about 450 bp apart. In order to immunoprecipitate, from the same DNA fragments, the proteins bound to both regions, nucleoprotein

complexes were sheared to reduce the length of DNA fragments to 500–1000 bp. In serial ChIP experiments, following primary immunoprecipitation, the cross-linked complexes were eluted from the immunoprecipitated fraction by incubation with elution buffer (1% SDS, 50 mM NaHCO₃) at room temperature for 30 min, and then diluted 1:10 in ChIP dilution buffer (0.01% SDS; 1.1% Triton X-100, 1.2 mM EDTA, 16.7 mM Tris-HCl, pH 8.0, 167 mM NaCl) followed by reimmunoprecipitation with a second set of antibodies.

Transient MBD2 siRNA knockdown and ER α vector transfections

siRNA duplexes for *MBD2* (sense: 5'-GGAGGAAGUGUACC-GAAATT-3'; antisense: 5'-UUUUCGGAUCACUCCUCCT-T-3') and non-specific siRNA control were obtained from Eurogentec (Eurogentec, Seraing, Belgium). HEG0, an expression vector coding for human ER α [31], and the empty vector pSG5, were provided by Prof. P. Chambon. MBD2 siRNA and ER α vector was transfected with Lipofectamine 2000 (Invitrogen, Carlsbad, CA) according to the manufacturer's instructions. Briefly, cells were seeded at 2×10^5 cells per well in six-well plates, and grown to 50–60% confluence on the day of transfection. All transfections were done in Opti-MEM medium (Invitrogen) with 625 nM of MBD2 siRNA and 1 μ g of ER α expression plasmid. Lipofectamine 2000 complexes were incubated for 4–5 hours. The medium was then removed and replaced with fresh medium. Cells were grown and harvested at various times after the transfection.

Reverse-transcription-PCR analysis

Total RNA was extracted from the cell lines using the RNeasy Mini kit (Qiagen). After extraction, the integrity of total RNA was examined on a 1.2% agarose gel containing 1 μ g/ml ethidium bromide and quantified by densitometry using a Fluor's fluorimeter and Quantity One software (Biorad, Ivry, France) by comparison with serial dilutions of a standard RNA (Roche, Molecular Biochemicals, Maylan, France).

pS2 mRNA was detected by relative RT-PCR using primers described in Supplemental Table S1. Briefly, 0.1 μ g of total RNA were amplified simultaneously for *β -actin* and *pS2* using the One Step RT-PCR kit (Qiagen). After 30 min incubation at 50°C, RT was inactivated by heating at 95°C for 15 min. PCR amplification was then performed under the following conditions: 30 cycles, 30 s denaturation at 94°C, 1 min annealing at 55°C and 1.5 min extension at 72°C. PCR products were analyzed on a 2% agarose gel and quantified. The ratio between *pS2* and *β -actin* signals was then determined.

Real-time RT-PCR were also carried out to quantify *pS2* mRNA using LightCycler[®] RNA Master SYBR Green I One-Step RT-PCR mix on a LightCycler[®] 2.0 system according to the

manufacturer's instructions (Roche). *β -actin* mRNA was used as a reference. The primers sequences used for reverse-transcription-PCR are available in Supplemental Table S1.

MBD2 mRNA was quantified by competitive quantitative RT-PCR as previously described [32].

Supporting Information

Figure S1 MBD2 siRNA treatments, supplementary data. (A) MBD2 expression in MBD2 siRNA transfected cells. Bar chart representing the efficiency of MBD2 siRNA in HeLa, MCF7 and MDA MB231 in mock treated cells, the initial amount of MBD2 molecules / μ g of total RNA was: $7.4 \times 10^6 \pm 1.3 \times 10^6$, in HeLa cells; $5.8 \times 10^6 \pm 1 \times 10^6$, in MDA MB231 cells and $3.2 \times 10^6 \pm 0.6 \times 10^6$, in MCF7 cells. The efficiency of MBD2 siRNA was calculated from the MBD2 mRNA in treated cells compared with mock-treated cells. Each bar represents the mean \pm standard deviation of, at least, three independent analyses. (B) MBD1, MBD2 and MeCP2 protein quantifications in HeLa cells expressing transient MBD2 siRNA. HeLa cells were pretreated for 72 h with MBD2 siRNA and again for 24 h. Mock-treated cells were transfected with a non-specific siRNA. Immunoblot analysis of MBD2, MBD1 and MeCP2 proteins in mock-treated and in MBD2 siRNA-treated HeLa cells. MBD2, MBD1 and MeCP2 proteins were probed using rabbit polyclonal antibodies. The same membrane was then stripped and probed using a mouse β -tubulin antibody as a loading control. (C) Bar chart showing the fold change of pS2 expression in MCF7 and MDA MB231 cells depleted in MBD2. pS2 transcripts were quantified by real-time RT-PCR. The fold change was calculated from the amount of pS2 mRNA in treated cells compared with mock-treated cells. Each bar represents the mean \pm standard deviation of, at least, three independent analyses.

Found at: doi:10.1371/journal.pone.0009665.s001 (0.52 MB TIF)

Table S1 List of primers.

Found at: doi:10.1371/journal.pone.0009665.s002 (0.03 MB DOC)

Acknowledgments

We thank Prof. Pierre Chambon for critical reading of this manuscript and his help with this project.

Author Contributions

Conceived and designed the experiments: AC EB RD. Performed the experiments: AC. Analyzed the data: AC EB ME. Contributed reagents/materials/analysis tools: AC EB ME. Wrote the paper: AC EB ME RD.

References

- Ehrlich M (2002) DNA methylation in cancer: too much, but also too little. *Oncogene* 21: 5400–5413.
- Esteller M (2007) Cancer epigenomics: DNA methylomes and histone-modification maps. *Nat Rev Genet* 8: 286–298.
- Baylin SB, Ohm JE (2006) Epigenetic gene silencing in cancer - a mechanism for early oncogenic pathway addiction? *Nat Rev Cancer* 6: 107–116.
- Masiakowski P, Breathnach R, Bloch J, Gannon F, Krust A, et al. (1982) Cloning of cDNA sequences of hormone-regulated genes from the MCF-7 human breast cancer cell line. *Nucleic Acids Res* 10: 7895–7903.
- Brown AM, Jeltsch JM, Roberts M, Chambon P (1984) Activation of pS2 gene transcription is a primary response to estrogen in the human breast cancer cell line MCF-7. *Proc Natl Acad Sci U S A* 81: 6344–6348.
- Amiry N, Kong X, Muniraj N, Kannan N, Grandison PM, et al. (2009) Trefoil factor-1 (TFF1) enhances oncogenicity of mammary carcinoma cells. *Endocrinology* 150: 4473–4483.
- Perry JK, Kannan N, Grandison PM, Mitchell MD, Lobie PE (2008) Are trefoil factors oncogenic? *Trends Endocrinol Metab* 19: 74–81.
- Martin V, Ribieras S, Song-Wang XG, Lasne Y, Frappart L, et al. (1997) Involvement of DNA methylation in the control of the expression of an estrogen-induced breast-cancer-associated protein (pS2) in human breast cancers. *J Cell Biochem* 65: 95–106.
- Dietrich D, Lesche R, Tetzner R, Krispin M, Dietrich J, et al. (2009) Analysis of DNA methylation of multiple genes in microdissected cells from formalin-fixed and paraffin-embedded tissues. *J Histochem Cytochem* 57: 477–489.
- Cedar H (1988) DNA methylation and gene activity. *Cell* 53: 3–4.
- Huang LH, Wang R, Gama-Sosa MA, Shenoy S, Ehrlich M (1984) A protein from human placental nuclei binds preferentially to 5-methylcytosine-rich DNA. *Nature* 308: 293–295.
- Meehan RR, Lewis JD, McKay S, Kleiner EL, Bird AP (1989) Identification of a mammalian protein that binds specifically to DNA containing methylated CpGs. *Cell* 58: 499–507.

13. Keshet I, Lieman-Hurwitz J, Cedar H (1986) DNA methylation affects the formation of active chromatin. *Cell* 44: 535–543.
14. Hendrich B, Bird A (1998) Identification and characterization of a family of mammalian methyl-CpG binding proteins. *Mol Cell Biol* 18: 6538–6547.
15. Bird AP, Wolffe AP (1999) Methylation-induced repression—belts, braces, and chromatin. *Cell* 99: 451–454.
16. Fatemi M, Wade PA (2006) MBD family proteins: reading the epigenetic code. *J Cell Sci* 119: 3033–3037.
17. Klose RJ, Bird AP (2006) Genomic DNA methylation: the mark and its mediators. *Trends Biochem Sci* 31: 89–97.
18. Saito M, Ishikawa F (2002) The mCpG-binding domain of human MBD3 does not bind to mCpG but interacts with NuRD/Mi2 components HDAC1 and MTA2. *J Biol Chem* 277: 35434–35439.
19. Wade PA, Geggion A, Jones PL, Ballestar E, Aubry F, et al. (1999) Mi-2 complex couples DNA methylation to chromatin remodelling and histone deacetylation. *Nat Genet* 23: 62–66.
20. Zhang Y, Ng HH, Erdjument-Bromage H, Tempst P, Bird A, et al. (1999) Analysis of the NuRD subunits reveals a histone deacetylase core complex and a connection with DNA methylation. *Genes Dev* 13: 1924–1935.
21. Hendrich B, Hardeband U, Ng HH, Jiricny J, Bird A (1999) The thymine glycosylase MBD4 can bind to the product of deamination at methylated CpG sites. *Nature* 401: 301–304.
22. Delaval K, Feil R (2004) Epigenetic regulation of mammalian genomic imprinting. *Curr Opin Genet Dev* 14: 188–195.
23. Barr H, Hermann A, Berger J, Tsai HH, Adie K, et al. (2007) Mbd2 contributes to DNA methylation-directed repression of the Xist gene. *Mol Cell Biol* 27: 3750–3757.
24. Jaenisch R, Bird A (2003) Epigenetic regulation of gene expression: how the genome integrates intrinsic and environmental signals. *Nat Genet* 33 Suppl. pp 245–254.
25. Lorincz MC, Dickerson DR, Schmitt M, Groudine M (2004) Intragenic DNA methylation alters chromatin structure and elongation efficiency in mammalian cells. *Nat Struct Mol Biol* 11: 1068–1075.
26. Auriol E, Billard LM, Magdinier F, Dante R (2005) Specific binding of the methyl binding domain protein 2 at the BRCA1-NBR2 locus. *Nucleic Acids Res* 33: 4243–4254.
27. Boyes J, Bird A (1992) Repression of genes by DNA methylation depends on CpG density and promoter strength: evidence for involvement of a methyl-CpG binding protein. *Embo J* 11: 327–333.
28. Curradi M, Izzo A, Badaracco G, Landsberger N (2002) Molecular mechanisms of gene silencing mediated by DNA methylation. *Mol Cell Biol* 22: 3157–3173.
29. Rio MC, Bellocq JP, Gairard B, Rasmussen UB, Krust A, et al. (1987) Specific expression of the pS2 gene in subclasses of breast cancers in comparison with expression of the estrogen and progesterone receptors and the oncogene ERBB2. *Proc Natl Acad Sci U S A* 84: 9243–9247.
30. Perrin D, Ballestar E, Fraga MF, Frappart L, Esteller M, et al. (2007) Specific hypermethylation of LINE-1 elements during abnormal overgrowth and differentiation of human placenta. *Oncogene* 26: 2518–2524.
31. Metzger D, Berry M, Ali S, Chambon P (1995) Effect of antagonists on DNA binding properties of the human estrogen receptor in vitro and in vivo. *Mol Endocrinol* 9: 579–591.
32. Billard LM, Magdinier F, Lenoir GM, Frappart L, Dante R (2002) MeCP2 and MBD2 expression during normal and pathological growth of the human mammary gland. *Oncogene* 21: 2704–2712.
33. Nunez AM, Berry M, Imler JL, Chambon P (1989) The 5' flanking region of the pS2 gene contains a complex enhancer region responsive to oestrogens, epidermal growth factor, a tumour promoter (TPA), the c-Ha-ras oncoprotein and the c-jun protein. *Embo J* 8: 823–829.
34. Metivier R, Penot G, Hubner MR, Reid G, Brand H, et al. (2003) Estrogen receptor- α directs ordered, cyclical, and combinatorial recruitment of cofactors on a natural target promoter. *Cell* 115: 751–763.
35. Metivier R, Penot G, Carmouche RP, Hubner MR, Reid G, et al. (2004) Transcriptional complexes engaged by apo-estrogen receptor- α isoforms have divergent outcomes. *Embo J* 23: 3653–3666.
36. Zinn RL, Pruitt K, Eguchi S, Baylin SB, Herman JG (2007) hTERT is expressed in cancer cell lines despite promoter DNA methylation by preservation of unmethylated DNA and active chromatin around the transcription start site. *Cancer Res* 67: 194–201.
37. Renaud S, Loukinov D, Abdullaev Z, Guilleret I, Bosman FT, et al. (2007) Dual role of DNA methylation inside and outside of CTCF-binding regions in the transcriptional regulation of the telomerase hTERT gene. *Nucleic Acids Res* 35: 1245–1256.
38. Sahar S, Sassone-Corsi P (2007) Circadian clock and breast cancer: a molecular link. *Cell Cycle* 6: 1329–1331.
39. Garcia-Bassets I, Kwon YS, Telesse F, Prefontaine GG, Hutt KR, et al. (2007) Histone methylation-dependent mechanisms impose ligand dependency for gene activation by nuclear receptors. *Cell* 128: 505–518.
40. Magdinier F, Wolffe AP (2001) Selective association of the methyl-CpG binding protein MBD2 with the silent p14/p16 locus in human neoplasia. *Proc Natl Acad Sci U S A* 98: 4990–4995.
41. Nguyen CT, Gonzales FA, Jones PA (2001) Altered chromatin structure associated with methylation-induced gene silencing in cancer cells: correlation of accessibility, methylation, MeCP2 binding and acetylation. *Nucleic Acids Res* 29: 4598–4606.
42. Lopez-Serra L, Ballestar E, Fraga MF, Alaminos M, Setien F, et al. (2006) A Profile of Methyl-CpG Binding Domain Protein Occupancy of Hypermethylated Promoter CpG Islands of Tumor Suppressor Genes in Human Cancer. *Cancer Res* 66: 8342–8346.
43. Ballestar E, Paz MF, Valle L, Wei S, Fraga MF, et al. (2003) Methyl-CpG binding proteins identify novel sites of epigenetic inactivation in human cancer. *Embo J* 22: 6335–6345.
44. Martin V, Ribieras S, Rio MC, Dante R (1998) The estrogen responsive element of the pS2 gene is recognized by a methylation sensitive DNA binding protein. *Biol Chem* 379: 409–416.
45. Giamarchi C, Solanas M, Chailleux C, Augereau P, Vignon F, et al. (1999) Chromatin structure of the regulatory regions of pS2 and cathepsin D genes in hormone-dependent and -independent breast cancer cell lines. *Oncogene* 18: 533–541.
46. Pao MM, Tsutsumi M, Liang G, Uzvolgyi E, Gonzales FA, et al. (2001) The endothelin receptor B (EDNRB) promoter displays heterogeneous, site specific methylation patterns in normal and tumor cells. *Hum Mol Genet* 10: 903–910.
47. Kangaspeska S, Stride B, Metivier R, Polycarpou-Schwarz M, Ibberson D, et al. (2008) Transient cyclical methylation of promoter DNA. *Nature* 452: 112–115.
48. Metivier R, Gallais R, Tiffoche C, Le Peron C, Jurkowska RZ, et al. (2008) Cyclical DNA methylation of a transcriptionally active promoter. *Nature* 452: 45–50.
49. Probst AV, Dunleavy E, Almouzni G (2009) Epigenetic inheritance during the cell cycle. *Nat Rev Mol Cell Biol* 10: 192–206.
50. Morgan HD, Santos F, Green K, Dean W, Reik W (2005) Epigenetic reprogramming in mammals. *Hum Mol Genet* 14 Spec No 1: R47–58.
51. Jin SG, Guo C, Pfeifer GP (2008) GADD45A does not promote DNA demethylation. *PLoS Genet* 4: e1000013.
52. Barreto G, Schafer A, Marhold J, Stach D, Swaminathan SK, et al. (2007) Gadd45a promotes epigenetic gene activation by repair-mediated DNA demethylation. *Nature* 445: 671–675.
53. Ooi SK, Bestor TH (2008) The colorful history of active DNA demethylation. *Cell* 133: 1145–1148.
54. Martiniowich K, Hattori D, Wu H, Fouse S, He F, et al. (2003) DNA methylation-related chromatin remodeling in activity-dependent BDNF gene regulation. *Science* 302: 890–893.
55. Chen WG, Chang Q, Lin Y, Meissner A, West AE, et al. (2003) Derepression of BDNF transcription involves calcium-dependent phosphorylation of MeCP2. *Science* 302: 885–889.
56. Hutchins AS, Mullen AC, Lee HW, Sykes KJ, High FA, et al. (2002) Gene silencing quantitatively controls the function of a developmental trans-activator. *Mol Cell* 10: 81–91.